

Mechanical Kerr nonlinearities due to bipolar optical forces between deformable silicon waveguides

Jing Ma* and Michelle L. Povinelli

Ming Hsieh Department of Electrical Engineering, University of Southern California, Powell Hall of Engineering,
3737 Watt Way, Los Angeles, California 90089-0271, USA

*jingm@usc.edu

Abstract: We use an analytical method based on the perturbation of effective index at fixed frequency to calculate optical forces between silicon waveguides. We use the method to investigate the mechanical Kerr effect in a coupled-waveguide system with bipolar forces. We find that a positive mechanical Kerr coefficient results from either an attractive or repulsive force. An enhanced mechanical Kerr coefficient several orders of magnitude larger than the intrinsic Kerr coefficient is obtained in waveguides for which the optical mode approaches the air light line, given appropriate design of the waveguide dimensions.

©2011 Optical Society of America

OCIS codes: (190.0190) Nonlinear optics; (130.0130) Integrated optics.

References and links

1. M. L. Povinelli, M. Ibanescu, S. G. Johnson, and J. D. Joannopoulos, "Slow-light enhancement of radiation pressure in an omnidirectional-reflector waveguide," *Appl. Phys. Lett.* **85**(9), 1466–1468 (2004).
2. M. L. Povinelli, M. Loncar, M. Ibanescu, E. J. Smythe, S. G. Johnson, F. Capasso, and J. D. Joannopoulos, "Evanescent-wave bonding between optical waveguides," *Opt. Lett.* **30**(22), 3042–3044 (2005).
3. A. Mizrahi, and L. Schächter, "Mirror manipulation by attractive and repulsive forces of guided waves," *Opt. Express* **13**(24), 9804–9811 (2005).
4. J. Ng, C. T. Chan, P. Sheng, and Z. Lin, "Strong optical force induced by morphology-dependent resonances," *Opt. Lett.* **30**(15), 1956–1958 (2005).
5. M. L. Povinelli, S. G. Johnson, M. Loncar, M. Ibanescu, E. Smythe, F. Capasso, and J. D. Joannopoulos, "High-Q enhancement of attractive and repulsive optical forces between coupled whispering-gallery-mode resonators," *Opt. Express* **13**(20), 8286–8295 (2005).
6. P. T. Rakich, M. A. Popovic, M. Soljacic, and E. P. Ippen, "Trapping, corralling and spectral bonding of optical resonances through optically induced potentials," *Nat. Photonics* **1**(11), 658–665 (2007).
7. H. Taniyama, M. Notomi, E. Kuramochi, T. Yamamoto, Y. Yoshikawa, Y. Torii, and T. Kuga, "Strong radiation force induced in two-dimensional photonic crystal slab cavities," *Phys. Rev. B* **78**(16), 165129 (2008).
8. D. Van Thourhout, and J. Roels, "Optomechanical device actuation through the optical gradient force," *Nat. Photonics* **4**(4), 211–217 (2010).
9. F. Riboli, A. Recati, M. Antezza, and I. Carusotto, "Radiation induced force between two planar waveguides," *Eur. Phys. J. D* **46**(1), 157–164 (2008).
10. M. Li, W. H. P. Pernice, and H. X. Tang, "Tunable bipolar optical interactions between guided lightwaves," *Nat. Photonics* **3**(8), 464–468 (2009).
11. G. S. Wiederhecker, L. Chen, A. Gondarenko, and M. Lipson, "Controlling photonic structures using optical forces," *Nature* **462**(7273), 633–636 (2009).
12. M. Li, W. H. P. Pernice, C. Xiong, T. Baehr-Jones, M. Hochberg, and H. X. Tang, "Harnessing optical forces in integrated photonic circuits," *Nature* **456**(7221), 480–484 (2008).
13. P. T. Rakich, M. A. Popović, and Z. Wang, "General treatment of optical forces and potentials in mechanically variable photonic systems," *Opt. Express* **17**(20), 18116–18135 (2009).
14. J. Roels, I. De Vlamincck, L. Lagae, B. Maes, D. Van Thourhout, and R. Baets, "Tunable optical forces between nanophotonic waveguides," *Nat. Nanotechnol.* **4**(8), 510–513 (2009).
15. M. Eichenfield, C. P. Michael, R. Perahia, and O. Painter, "Actuation of micro-optomechanical systems via cavity-enhanced optical dipole forces," *Nat. Photonics* **1**(7), 416–422 (2007).
16. J. Rosenberg, Q. Lin, and O. Painter, "Static and dynamic wavelength routing via the gradient optical force," *Nat. Photonics* **3**(8), 478–483 (2009).

17. J. Ma, and M. L. Povinelli, "Large tuning of birefringence in two strip silicon waveguides via optomechanical motion," *Opt. Express* **17**(20), 17818–17828 (2009).
 18. J. Ma, and M. L. Povinelli, "Effect of periodicity on optical forces between a one-dimensional periodic photonic crystal waveguide and an underlying substrate," *Appl. Phys. Lett.* **97**(15), 151102 (2010).
 19. P. Meystre, E. M. Wright, J. D. McCullen, and E. Vignes, "Theory of radiation-pressure-driven interferometers," *J. Opt. Soc. Am. B* **2**(11), 1830–1840 (1985).
 20. W. H. P. Pernice, M. Li, and H. X. Tang, "A mechanical Kerr effect in deformable photonic media," *Appl. Phys. Lett.* **95**(12), 123507 (2009).
 21. S. G. Johnson, and J. D. Joannopoulos, "Block-iterative frequency-domain methods for Maxwell's equations in a planewave basis," *Opt. Express* **8**(3), 173–190 (2001).
 22. J. D. Jackson, *Classical Electrodynamics* (Wiley, 1999).
 23. W. H. P. Pernice, M. Li, and H. X. Tang, "Theoretical investigation of the transverse optical force between a silicon nanowire waveguide and a substrate," *Opt. Express* **17**(3), 1806–1816 (2009).
 24. S. Timoshenko, *Theory of Elasticity* (McGraw-Hill, 1934).
 25. M. Soljacić, C. Luo, J. D. Joannopoulos, and S. Fan, "Nonlinear photonic crystal microdevices for optical integration," *Opt. Lett.* **28**(8), 637–639 (2003).
-

1. Introduction

In the last few years, intense research has been carried out on optical forces induced by the strongly enhanced gradient of the electromagnetic field close to micro- and nanophotonic devices [1–14]. Optical forces provide a novel way to tune the properties of microphotonic devices by changing the separation between their components. This mechanical actuation allows a number of important device functionalities, such as all-optically controlled filters [15], wavelength routers [16], polarization rotators [17], and power limiters [18].

It has previously been suggested that optomechanical coupling in macroscale Fabry-Perot cavities can be viewed as an effective nonlinearity [19]. The concept can be generalized to other types of devices that move in response to optical forces. A mechanical Kerr effect has been predicted in a microphotonic Si waveguide with a suspended, movable section [20]. The mechanical Kerr coefficient n_2^m is several orders of magnitude larger than the intrinsic Kerr coefficient of silicon. The origin of the mechanical Kerr effect lies in optical coupling between the waveguide and substrate. Coupling results in an attractive optical force that pulls the waveguide closer to the substrate, changing the effective index of the waveguide mode. Since the optical force is proportional to the optical power in the waveguide, the shift in effective index depends on intensity; for this system, the mechanical Kerr coefficient is positive.

It is intriguing to explore whether microphotonic devices can be designed to tailor the value and sign of the mechanical Kerr coefficient, yielding "customizable" nonlinear materials. In this paper, we examine a coupled, two-waveguide system in which the forces can be either attractive or repulsive. We show that the mechanical Kerr coefficient scales as the optical force squared. As a result, the mechanical Kerr coefficient is positive for either an attractive or repulsive force. The force can be expressed as a derivative of the effective index with respect to separation at fixed frequency. We calculate the mechanical Kerr coefficient numerically for varying waveguide cross sections. We find that n_2^m is greatest when the modes are neither too delocalized nor too confined in deformable waveguides. Under these conditions, the force which is enhanced by strong evanescent-wave coupling and the increased displacement give rise to the largest shift in effective index.

2. Coupled waveguides exhibiting bipolar optical forces

We consider the coupled waveguides shown in Fig. 1(a). Two parallel, silicon strip waveguides (refractive index $n = 3.45$) are separated by a distance d . Both ends of the waveguides rest on a SiO₂ (refractive index $n = 1.5$) substrate. The suspended section has length L . Each waveguide has a cross section of dimensions $w \times h$. From previous work [2], it is known that optical coupling between the waveguides gives rise to a mechanical force. The magnitude of the force is proportional to the optical power, and the sign is either attractive or

repulsive, depending on the relative phase of light in the two waveguides. The force per unit length in the suspended section can be calculated from the full-vectorial eigenmodes of the coupled waveguides using the Maxwell Stress Tensor method, as in Ref [2].

Figure 1(b) shows the dispersion relation for the two lowest-order modes that have an electric field primarily in the z -direction. Calculations were performed using the MIT Photonic Bands (MPB) package [21]. To illustrate the dependence on waveguide separation, the dispersion relation is plotted for a smaller (100nm) and larger (1000nm) value of separation d . For the lowest mode, the electric field component E_z is symmetric in the two waveguides. The symmetric mode corresponds to an attractive force. Decreasing separation shifts the dispersion relation to a larger k value, in the direction shown by the blue, solid arrow. For the second lowest mode, E_z is antisymmetric and the force is repulsive. Increasing separation also shifts the dispersion relation to larger k value, in the direction shown by the blue, dashed arrow. Below, we relate the shift in dispersion relation at fixed frequency to the optical force.

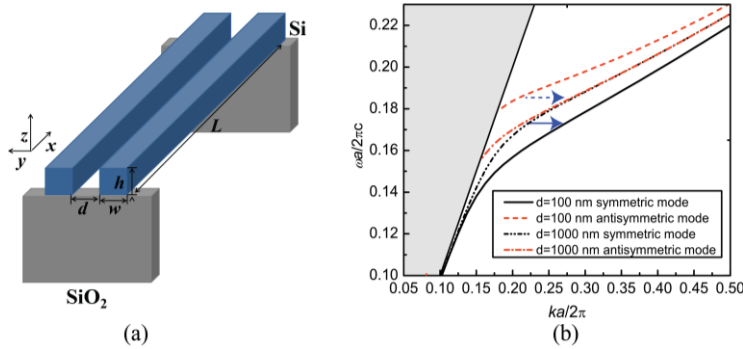


Fig. 1. (a) Two coupled silicon waveguides, each with cross section $w \times h$, separated by a distance d and resting on a SiO_2 substrate with suspended length L . (b) Dispersion relation for modes of the suspended section. The two lowest modes with electric field vectors primarily in the z -direction are plotted for separations $d = 100 \text{ nm}$ and $d = 1000 \text{ nm}$. The cross section of each waveguide is $350 \times 350 \text{ nm}^2$. The gray region shows the light cone for air.

Figure 2 introduces notation to describe the shift in dispersion relation $\omega(k)$ resulting from a small change in waveguide separation δd . The solid and dashed lines are the initial and shifted bands, respectively. For constant frequency operation at frequency ω_0 , the magnitude of the wave vector shifts from k_0 to k_2 . If we consider a constant wave vector k_0 , the dispersion relation shifts from ω_0 to ω_1 .

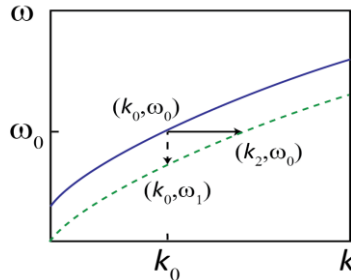


Fig. 2. Schematic diagram showing a shift in the dispersion relation due to a change in separation between waveguides d . The solid and dashed lines represent the initial and shifted dispersion relation, respectively.

3. Calculation of optical force

For infinitely long waveguides with no radiation loss, the optical force may be calculated as a derivative of the eigenmode frequency with respect to separation [2]:

$$\frac{F}{LP} = -\frac{1}{c} \frac{n_g}{\omega} \frac{\partial \omega}{\partial d} \Big|_k, \quad (1)$$

where $F/(LP)$ represents the force per length per unit power, n_g is the group index, and c is the speed of light in vacuum. Note that the derivative is taken at constant k . Equation (1) has been shown to agree well with direct calculations via the Maxwell Stress Tensor (MST) [22] for the coupled waveguide system [2].

By substituting $\omega = ck/n_{\text{eff}}$ into Eq. (1), the force may alternately be expressed as a function of the effective index n_{eff} [23]:

$$\frac{F}{LP} = \frac{1}{c} \frac{n_g}{n_{\text{eff}}} \frac{\partial n_{\text{eff}}}{\partial d} \Big|_k. \quad (2)$$

We may recast the force in terms of a derivative at fixed frequency as follows. As shown by the dashed arrow in Fig. 2, for fixed wave vector k_0 , a small change in separation δd moves the eigenmode from (k_0, ω_0) to (k_0, ω_1) , corresponding to a shift of n_{eff} :

$$\delta n_{\text{eff}} \Big|_k = ck_0 \left(\frac{1}{\omega_1} - \frac{1}{\omega_0} \right) = ck_0 \frac{-\delta\omega}{(\omega_0 + \delta\omega)\omega_0}, \quad (3)$$

where $\delta\omega = \omega_1 - \omega_0$. For fixed frequency ω_0 , the shift of the dispersion relation changes the wave vector from k_0 to k_2 . The change of n_{eff} for fixed ω is:

$$\delta n_{\text{eff}} \Big|_\omega = \frac{c}{\omega_0} (k_2 - k_0) = \frac{c}{\omega_0} \delta k, \quad (4)$$

where $\delta k = k_2 - k_0$. By comparing Eq. (3) and (4), we find:

$$\frac{\delta n_{\text{eff}} \Big|_k}{\delta n_{\text{eff}} \Big|_\omega} = -\frac{\delta\omega}{\delta k} \frac{k_0}{(\omega_0 + \delta\omega)} \approx -\frac{\delta\omega}{\delta k} \frac{k_0}{\omega_0}. \quad (5)$$

If the band is shifted by a small amount, the ratio $\delta\omega/\delta k$ can be estimated by $-c/n_g$. (The negative sign results from the fact that $\delta\omega = \omega_1 - \omega_0$ is defined to be negative in Fig. 2.) Eq. (5) can then be rewritten as:

$$\frac{\delta n_{\text{eff}} \Big|_k}{\delta n_{\text{eff}} \Big|_\omega} \approx \frac{n_{\text{eff}}}{n_g}. \quad (6)$$

For finite shift, Eq. (2) can be approximated by

$$\frac{F}{LP} \approx \frac{1}{c} \frac{n_g}{n_{\text{eff}}} \frac{\delta n_{\text{eff}}}{\delta d} \Big|_k. \quad (7)$$

Substituting Eq. (6) into Eq. (7) and taking the limit as $\delta d \rightarrow 0$ yields the result

$$\frac{F}{LP} = \frac{1}{c} \frac{\partial n_{\text{eff}}}{\partial d} \Big|_\omega, \quad (8)$$

showing that the optical force can be calculated in terms of the effective index $n_{\text{eff}}(d)$ at a fixed optical frequency. Negative values here correspond to attractive forces. Ref [13]. used a different derivation, based on energy and photon-number conservation, to arrive at the same expression.

We compared force values calculated with Eq. (8) to those calculated using the MST method. The wavelength was fixed to 1550 nm and the waveguide dimensions to $h = w = 350$ nm. The derivative in Eq. (8) was approximated as a finite difference, using values of $n_{\text{eff}}(d)$ calculated with the MPB package. Figure 3(a) shows $n_{\text{eff}}(d)$ for the symmetric mode (black

line). The force calculated using Eq. (8) is plotted in Fig. 3(a) (red triangles). It agrees well with the force calculated using the MST method (red curve). The MST was evaluated using the full vectorial eigenmodes obtained from MPB. As predicted by Eq. (8), the force is attractive (negative), corresponding to a decreasing $n_{\text{eff}}(d)$.

Figure 3(b) shows n_{eff} (black curve) and $F/(LP)$ for the antisymmetric mode. Forces calculated by Eq. (8) (red triangles) agree well with values calculated using the MST method (red curve). Note that the value of n_{eff} first decreases and then increases as a function of d . Correspondingly, the derivative $\partial n_{\text{eff}} / \partial d|_{\omega}$ turns from negative to positive, and the optical force changes from negative (attractive) to positive (repulsive) as a function of separation. We emphasize that the sign of the force can be easily inferred from the slope of n_{eff} .

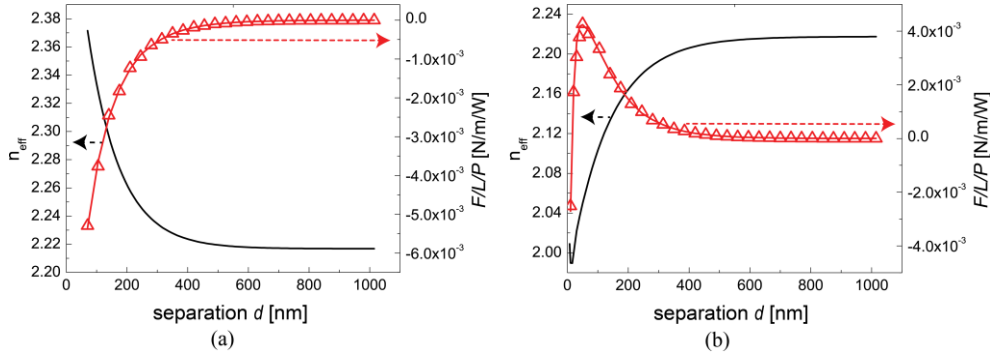


Fig. 3. For fixed wavelength 1550 nm and waveguide dimensions $h = w = 350$ nm: (a) Symmetric mode: n_{eff} as a function of d (black curve); $F/(LP)$ calculated by the MST method (red curve) and by Eq. (8) (red triangles). (b) Antisymmetric mode: n_{eff} as a function of d (black curve); $F/(LP)$ calculated by the MST method (red curve) and by Eq. (8) (red triangles).

4. Calculation of Mechanical Kerr coefficient

The mechanical Kerr effect arises from the change in effective index due to waveguide deformation. We consider static deformations. The optical force between the waveguides is proportional to the power, P , and causes the waveguides to deform. For the symmetric mode, the force is attractive and the waveguides are pulled together. For the antisymmetric mode, the force is repulsive and the waveguides are pushed apart. The maximum deformation will be at the center of the waveguide, since the ends of the waveguides are fixed to the silica substrate. We consider the case where the deformation is small compared to the initial separation. The magnitude of the deformation is also much smaller than the length of the suspended region, L . Under deformation, the effective index n_{eff} varies along the length of the waveguides, according to the local separation. Following Ref [10], we define the mechanical Kerr coefficient n_2^m through the relation $\Delta n_{\text{eff}}(I) = n_2^m I$, where $\Delta n_{\text{eff}}(I)$ is the change in the effective index at the center of the suspended region, and I is the light intensity. Specifically, we take $I = P/A$, where A is the mode area, equal to $(\iint \varepsilon(y, z) |E|^2 dy dz) / \max(\varepsilon |E|^2)$.

Using Eq. (8), which relates the force to the derivative of the effective index with respect to separation, we can show that either an attractive or repulsive force gives rise to a positive mechanical Kerr coefficient. Figure 3(a) shows that for the symmetric mode, n_{eff} decreases with d . From Eq. (8), the force is negative (attractive) and pulls the waveguides closer together. The separation at the center of the suspended length decreases, resulting in an increase in n_{eff} . The mechanical Kerr coefficient n_2^m is thus positive. For the antisymmetric mode, in the region where n_{eff} decreases with d , the same argument shows that n_2^m is positive. In the region where n_{eff} increases with d , the force is positive (repulsive), which increases the

separation at the center of the suspended region and increases n_{eff} . Again, a positive mechanical Kerr coefficient n_2^m is obtained.

The mechanical Kerr coefficient can be evaluated numerically from the value of the optical force. When the deformation is small with respect to the initial separation, the change of the effective index for a signal with fixed frequency can be approximated by:

$$\Delta n_{\text{eff}} = \Delta d \times \left. \frac{\partial n_{\text{eff}}}{\partial d} \right|_{\omega}, \quad (9)$$

where Δd is the change in separation, equal to twice the deformation of a single waveguide, which can be modeled as a double-clamped beam [24]:

$$\Delta d = 2 \times \left(FL^3 / 32Ehw^3 \right), \quad (10)$$

where E is the Young's modulus of silicon. By manipulating Eq. (8), (9) and (10), we get

$$\Delta n_{\text{eff}} = \frac{1}{c} \left(\left. \frac{\partial n_{\text{eff}}}{\partial d} \right|_{\omega} \right)^2 \frac{PL^4}{16Ehw^3}, \quad (11)$$

or

$$\Delta n_{\text{eff}} = c \left(\frac{F}{LP} \right)^2 \frac{PL^4}{16Ehw^3}. \quad (12)$$

The mechanical Kerr coefficient is

$$n_2^m = \frac{\Delta n_{\text{eff}}}{I} = c \left(\frac{F}{LP} \right)^2 \frac{L^4}{16Ehw^3} A. \quad (13)$$

Note that $F/(LP)$ depends on the initial separation d and the waveguide cross section parameters, h and w . n_2^m also explicitly depends on the waveguide geometry parameters h , w , and L .

Note that Eq. (13) provides another means of seeing that both attractive and repulsive forces give positive mechanical Kerr coefficient: n_2^m depends on $(F/(LP))^2$.

4.1. Symmetric mode

In this subsection, we discuss how to design the waveguide cross section parameters h and w to enhance $F/(LP)$ and n_2^m for the symmetric mode. We set $\lambda = 1550$ nm, $L = 20$ μm , initial separation $d = 100$ nm, and $P = 10$ mW.

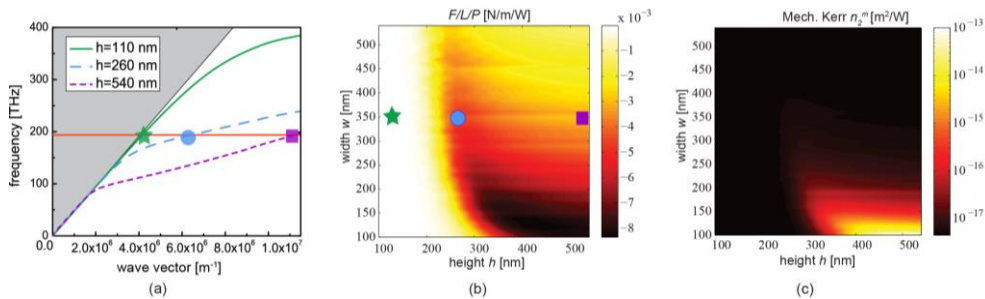


Fig. 4. Symmetric mode: (a) Band structure. The gray region represents the air light cone. The red line shows fixed wavelength 1550 nm (frequency 193.55 THz). (b) Attractive force per length per unit power $F/(LP)$. The initial separation $d = 100$ nm, suspended length $L = 20$ μm , optical power $P = 10$ mW, and the signal wavelength is 1550 nm. (c) Mechanical Kerr coefficient n_2^m .

Figure 4(b) shows $F/(LP)$ for the symmetric mode in waveguides with various heights and widths.

The strongest attractive force is shown by the darkest region, which corresponds to waveguides with large heights and small widths. To understand the mechanism behind the force enhancement, we plot the dispersion relation of the mode in Fig. 4(a). For a waveguide with $h = 260$ nm and $w = 350$ nm, marked by the circle in Fig. 4(b), $F/(LP)$ has a relatively large, negative value of -4.1×10^{-3} N/m/W. The corresponding point in the dispersion relation is below and close to the air light line, as indicated by the circle in Fig. 4(a).

Figure 4(b) shows that if the waveguide cross section is too large, the attractive force is decreased (yellow region). As marked by the square in Fig. 4(b), when $h = 540$ nm and $w = 350$ nm, $F/(LP)$ is reduced to -2.7×10^{-3} N/m/W. The mode in such a system is well below the air light line. The light is confined in the two waveguides, with minimal optical coupling between them, and the magnitude of the force is decreased.

The white region of Fig. 4(b) shows that when the waveguide cross section is too small, the force magnitude is less than 10^{-3} N/m/W. For example, $F/(LP)$ on the waveguide with $h = 110$ nm and $w = 350$ nm (marked by the star) is on the order of 10^{-5} N/m/W. Figure 4(a) shows that the mode is on the asymptote of the light line. The mode energy spreads into the surrounding air, giving rise to a small force. In order to achieve a larger attractive force, we can design the waveguide cross section to make the optical mode approach the air light line but not overlap with the light line, as indicated by the circle in Fig. 4(a).

The mechanical Kerr coefficient n_2^m can be determined from the force by using Eq. (13) and is shown in Fig. 4(c). The biggest n_2^m in Fig. 4(c) is over 40,000 times bigger than the intrinsic Kerr coefficient of silicon, equal to 4.5×10^{-18} m²/W. The value of n_2^m is largest when the optical force is strong and the waveguide width is small. A thin waveguide is more deformable to the optical force along the y direction. For example, $F/(LP)$ for a waveguide of $h = 400$ nm and $w = 200$ nm is -6.7×10^{-3} N/m/W, which has the same order of magnitude as $F/(LP) = -7.2 \times 10^{-3}$ N/m/W for a waveguide of $h = 400$ nm and $w = 100$ nm. However, by reducing w from 200 nm to 100 nm, we can increase n_2^m from 2.4×10^{-14} m²/W to 1.7×10^{-13} m²/W.

4.2. Antisymmetric mode

We calculated $F/(LP)$ and n_2^m for the antisymmetric mode for waveguides with various heights and widths. We only consider guided (non-leaky) modes, lying underneath the light cone.

Figure 5(b) shows $F/(LP)$. The force is positive (repulsive). The bright region indicates the combination of waveguide heights and widths that result in relatively large optical force for 1550-nm light. The blue curve indicates the conditions for mode cutoff: a guided mode exists only above and to the right of the curve. Large forces can be obtained by choosing cross-sectional parameters on the upper, right boundary of the curve. For example, for $h = 320$ nm and $w = 250$ nm, marked by the circle in Fig. 5(b), $F/(LP)$ is 9.5×10^{-3} N/m/W. The corresponding mode in the dispersion relation lies close to and below the light line, as indicated by the circle in Fig. 5(a).

The repulsive force decreases for waveguides with cross-sectional dimensions much larger than cutoff. As marked by the square in Fig. 5(b), when $h = 540$ nm and $w = 250$ nm, $F/(LP)$ is reduced to 5.7×10^{-3} N/m/W. The mode energy is confined in the waveguides, and the light intensity in the air gap is reduced, decreasing the optical force. If the waveguide cross-sectional dimension is too small, as marked by the star in Fig. 5(b) for $h = 110$ nm and $w = 250$ nm, the mode becomes leaky.

Figure 5(c) shows that the sign of n_2^m induced by a repulsive force is positive for various cross-sectional dimensions. In order to increase n_2^m , we should choose dimensions on the right boundary of the blue curve and reduce w to make the waveguides more deformable. For example, if we choose $h = 540$ nm and $w = 140$ nm, n_2^m is approximately 8.1×10^{-13} m²/W, which is more than 150,000 times larger than the intrinsic Kerr coefficient of silicon.

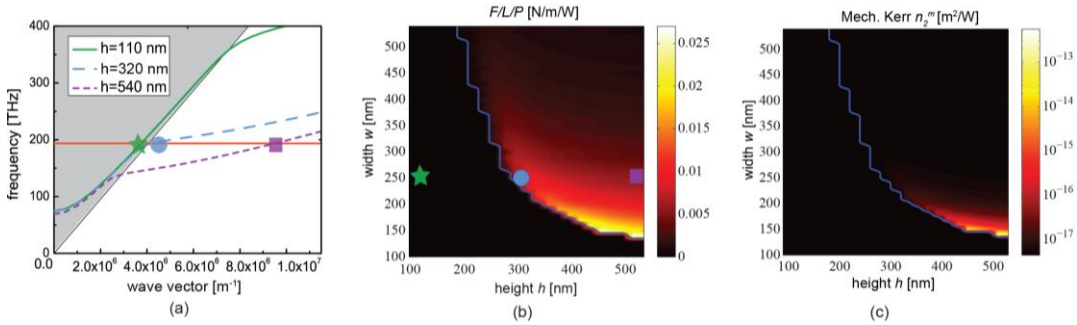


Fig. 5. Anti-symmetric mode: (a) Band structure. The gray region represents the air light cone. The red line shows fixed wavelength 1550 nm (frequency 193.55 THz). (b) Repulsive force per length per unit power $F/(LP)$. The initial separation $d = 100$ nm, suspended length $L = 20$ μ m, optical power $P = 10$ mW, and the signal wavelength is 1550 nm. (c) Mechanical Kerr coefficient n_2^m .

4.3. Discussion

Above, we have shown that for fixed waveguide length and initial separation, we can increase the mechanical Kerr coefficient n_2^m by adjusting the waveguide width and height. From Eqs. (8) and (9), we may infer that n_2^m is proportional to the product of the optical force F and the waveguide displacement Δd . The mechanical Kerr nonlinearity can thus be enhanced by i), increasing the optical force and ii), making the waveguide more deformable.

Figures 4(b) and 5(b) show that the force depends on waveguide cross-section dimensions. For either the symmetric or anti-symmetric modes, decreasing the waveguide height at fixed width shifts the mode closer to the light line. For the symmetric mode, the largest force is obtained when the mode is close to, but not too close to, the light line. For the anti-symmetric mode, the largest force is obtained when the mode approaches the cut-off geometry (blue line), where the mode crosses the light line. We may interpret both these conditions as meaning that the modes should be neither too delocalized in the surrounding air, nor too confined inside the waveguides, to optimize coupling between the waveguides and produce a large force. Meanwhile, the waveguide can also be made more deformable by adjusting waveguide dimensions. Equation (10) indicates that Δd is inversely proportional to hw^3 . Overall, the largest n_2^m values are obtained for small values of the width w (Figs. 4(c) and 5(c)).

We have presented results for both the symmetric and anti-symmetric mode. Both modes give positive mechanical Kerr coefficients n_2^m , and the maximum values are both on the order of 10^{-13} m²/W. Comparing Figs. 4(c) and 5(c), we observe that the symmetric mode has a bigger, brighter region representing n_2^m greater than 10^{-14} m²/W. In other words, to realize the same value of n_2^m , there is greater flexibility in waveguide dimensions using the symmetric mode. Another reason to choose the symmetric mode is that exciting the antisymmetric mode increases device complexity; for example, it has been demonstrated that a Mach-Zender

interferometer can be used to control the phase difference between light incident in the two waveguides [10,14].

Note that the optical frequency is many orders of magnitude larger than the mechanical resonance frequency, which is in the MHz range. Because the instantaneous optical force oscillates much faster than the mechanical motion, we consider the effect of the time-averaged, or “smoothed,” optical force on the waveguides, where the average is taken over the optical cycle. Assume the incident power is switched on and remains fixed. Driven by the optical force, the waveguides will start to deform. A steady-state displacement will be reached after a period of time proportional to the mechanical quality factor divided by the mechanical resonance frequency. In this paper, we focus on the static mechanical Kerr coefficient n_2^m caused by the steady-state displacement. However, for fixed power, larger displacements can be obtained by modulating the incident optical power at the mechanical resonance frequency [20]. The displacement will vary as a function of time throughout the period of mechanical vibration. At the peak displacement value, the instantaneous n_2^m reaches its maximum. n_2^m will be increased by a factor of Q_{mech} with respect to the case of static displacement, where Q_{mech} is the mechanical quality factor. However, if the average mechanical displacement is zero, the average value of n_2^m will also be zero.

5. Conclusion

We have investigated mechanical Kerr effects in a coupled-waveguide system exhibiting both attractive and repulsive forces. The optical force can be related to the change in effective index with separation at frequency. This formulation makes it clear that either an attractive or repulsive force gives rise to a positive mechanical Kerr coefficient. Values several orders of magnitude larger than the intrinsic Kerr coefficient are obtained for waveguides in which the optical mode approaches the air light line.

Since the mechanical Kerr effect results from physical motion, the time scale for response will be slower than for the intrinsic Kerr nonlinearity. At the same time, however, the magnitude is orders of magnitude larger. This suggests the potential for the design of ultra-low threshold, integrated optical devices such as all-optical transistors and isolators [25] that use the mechanical Kerr effect. Such devices might respond to the *average* power in an optical data stream, where the time-average is related to the time scale for mechanical response, and ultimately find use in the regulation of on-chip optical networks.

Acknowledgments

This work is supported by a National Science Foundation CAREER award under Grant No. 0846143. Computation for the work described in this paper was supported by the University of Southern California Center for High-Performance Computing and Communications (www.usc.edu/hpcc).